

1 2 9 0



UNIVERSIDADE D COIMBRA

Vasco Pedro Neto de Vasconcelos

Turbulence Infodynamics

Dissertation within the scope of the Masters in Mechanical Engineering supervised by Professor Doutor Miguel Rosa Oliveira Panão and presented to Department of Mechanical Engineering at the Faculty of Sciences and Technology

July of 2024

1 2



9 0

FACULDADE DE
CIÊNCIAS E TECNOLOGIA
UNIVERSIDADE DE
COIMBRA

Turbulence Infodynamics

Submitted in Partial Fulfilment of the Requirements for the
Degree of Master in Mechanical Engineering

Infodinâmica da Turbulência

Author

Vasco Pedro Neto de Vasconcelos

Supervisor

Miguel Rosa Oliveira Panão

Jury

President	Professor Doutor Eugénio Miguel de Sousa Rodrigues Assistant Professor at the University of Coimbra
Supervisor	Professor Doutor Miguel Rosa Oliveira Panão Assistant Professor at the University of Coimbra
Vowel	Professor Doutor Almerindo Domingues Ferreira Assistant Professor at the University of Coimbra

Coimbra, July, 2024

“Randomness is as necessary to physics as determinism.”
James P. Crutchfield

Acknowledgements

When I was a young boy, I used to say that when I grew up I wanted to become an "inventor". Now, about twenty years later, I find myself graduating from mechanical engineering, filled with motivation to begin my journey. I always knew I had an admiration for mathematics. The first big book I read was "O assassinato de Pitágoras" by Marcos Chicot, which perhaps was a big tell sign of my interest in the world of physics, how nature works, and how to use it.

This passion was then intensified while I was working on this dissertation. It gave me the opportunity to be part of and witness firsthand the making of science as we unravelled a bit of the world of turbulence. For this, I express my deepest gratitude to Professor Miguel Panão. His vote of confidence was invaluable, but even more so were the long conversations that not only fostered my technical understanding but also deepened my overall love for science.

I am also grateful to my parents. They have raised me in a way that I feel proud of myself, and so I see my achievements as theirs too.

Finally, to all those who have walked alongside me on this journey, your encouragement and support are deeply cherished. This gratitude is embodied in the very instrument used to write these Acknowledgements - a Typewriter, a gift from my late grandfather.

Thank you!

This is only the beginning of a journey...

Abstract

The complex, non-deterministic, and stochastic nature of turbulence is a puzzle that has long intrigued researchers. Its paramount importance in engineering cannot be overstated, as it holds significant implications for assessing performance in turbulent flows, for example, eventual losses in vertical/short take-off and landing aircraft. This research, which integrates principles of information theory, is a crucial step in our ongoing efforts to understand and harness the power of turbulence in engineering. The main goal of this dissertation is to test a novel lexicon in infodynamics, evaluating whether it offers or not a fresh perspective in the analysis of physical phenomena. Each new term introduced to the stochastic analysis of fluid flows offers a unique and innovative addition. **Informature**: a variable that quantifies the amount of information needed to learn about the inherent indeterminacy within a system's state. It offers deep insights into the system's diversity. **Infotropy**: a contextualized informature that measures the degree of transformation of a particular context associated with the physical system. **Infosensor**: an instrument or measurement technique able to capture enough information to measure informature through statistical analysis principles applied to the acquired data. Among the findings in this dissertation emerged a new perspective on turbulence intensity that overcomes its limitation at low-velocity values, transforming it into a turbulence intensity relative infotropy. Despite the many useful phenomena of turbulence in engineering that are yet to be thoroughly studied, one concludes that this informational approach opens promising avenues for a comprehensive understanding of their non-deterministic nature. More importantly, it unveils a myriad of potential applications that could introduce the impact of indeterminacy in engineering design.

Keywords: Turbulence, Infodynamics, Informature, Infotropy, Infosensor, Turbulence Intensity.

Resumo

A complexa, não-determinística e estocástica natureza da turbulência é um enigma que há muito intriga os investigadores. A sua importância capital na engenharia não pode ser subestimada, pois tem implicações significativas na avaliação do desempenho em escoamentos turbulentos, como, por exemplo, eventuais perdas em aeronaves de descolagem e aterragem vertical/curta. Esta investigação, que integra princípios da teoria da informação, é um passo crucial nos esforços contínuos para entender e aproveitar o valor da turbulência na engenharia. O principal objetivo desta dissertação consiste em testar um léxico inovador na infodinâmica, avaliando se oferece ou não uma perspetiva renovada na análise de fenómenos físicos. Cada novo termo introduzido na análise estocástica de escoamentos proporciona uma adição única e inovadora. Informatura: uma variável que quantifica a quantidade de informação necessária para aprender sobre a indeterminação inerente ao estado de um sistema, oferecendo uma compreensão profunda da diversidade do mesmo. Infotropia: uma informatura contextualizada que mede o grau de transformação de um determinado contexto associado a um sistema físico. Infosensor: um instrumento ou técnica de medida capaz de capturar informações suficientes para medir a informatura através de princípios de análise estatística aplicados aos dados adquiridos. Entre os resultados desta dissertação emergiu uma nova perspetiva sobre a intensidade da turbulência que pretende ultrapassar a sua limitação em valores de baixa velocidade, transformando-a numa infotropia relativa da intensidade de turbulência. Apesar dos muitos fenómenos úteis da turbulência na engenharia que ainda precisam de ser estudados exaustivamente, conclui-se que esta abordagem informacional abre vias promissoras para uma compreensão abrangente do seu impacto. Mais importante ainda, revela uma miríade de potenciais aplicações que podem introduzir o impacto da indeterminância no design em engenharia.

Palavras Chave: Turbulência, Infodinâmica, Informatura, Infotropia, Infosensor, Intensidade de Turbulência.

Contents

Acknowledgements	vii
Abstract	ix
Resumo	xi
Contents	xiii
List of Figures	xv
List of Tables	xvii
List of Abbreviations and Acronyms	xix
Nomenclature	xxi
1 Introduction	1
1.1 Objectives	2
1.2 Literature Review	3
2 Infodynamic Analysis Fundamentals	5
2.1 New Lexicon of Infodynamics	5
2.1.1 Informature	6
2.1.2 Infotropy	6
2.1.3 Mutual Informature	7
2.2 Calibrating Infosensors.	8
3 Infodynamic Analysis of Turbulence in Ground Vortex	13
3.1 Ground Vortex Velocity Characterization.	13
3.2 Informature Maps of Velocity fields	16
3.3 Turbulence Intensity Infotropy	18
4 Conclusions and Future Work	23
Bibliography	25
Appendices	26
A Laser Doppler Velocimetry System Details	27

List of Figures

2.1	Schematics of the message s and the random variable X that defines it.	6
2.2	Venn diagram of <i>mutual informature</i> between two messages, one described by the random variable X and the other by the random variable Y , interpreted from Stone (2015).	8
2.3	Evolution of <i>informature</i> , $H_{I,e}$, <i>differential informature</i> , $H_{\Delta,e}$, and the number of classes with the growth of the data sample size, N , by Panão (2024).	10
3.1	Diagram of the ground vortex facility by Barata et al. (2008).	13
3.2	Illustration of the three vortical rotation directions (ground vortex, secondary and small vortices). Detail of the intersection region where different tonalities in grey allow distinguishing the three vortices by Silva et al. (2017).	14
3.3	Small vortex burst and new vortex growth for $U_R = 1.74$. Frames instants: $t=0s$; $1/25s$; $2/25s$; $3/25s$. Figure taken from Barata et al. (2008).	14
3.4	Map of mean velocity regarding the vertical component, \bar{v} (left) and horizontal component, \bar{u} (right) superimposed with the corresponding streamlines from Barata et al. (2008).	15
3.5	Map of the average velocity fluctuations regarding the vertical component, v_{rms} (left) and horizontal component, u_{rms} (right) superimposed with the corresponding streamlines from Barata et al. (2008).	16
3.6	Example of the evolution of the <i>informature</i> , $H_{I,e}$, and <i>differential informature</i> , $H_{\Delta,e}$, relative to the velocity component u , v , as the data sample size (N) grows. This case corresponded to the LDV signal point for $Y = 60$ mm and $X = 0$ mm.	16
3.7	Obtained <i>informature</i> map regarding the v -velocity component (top) u -velocity component (bottom) and the corresponding calculated streamlines.	17
3.8	Evolution of the <i>informature</i> , $H_{I,e}$, relative to the velocity component u , v , and the <i>mutual informature</i> , $mH_{I,e}(u, v)$, as the data sample size, N , grows, by Panão (2024).	18
3.9	<i>Mutual informature</i> map between the horizontal, u , and vertical, v , velocity components.	18
3.10	Obtained results regarding turbulence intensity for the v -velocity component (left) and for the u -velocity component (right), and the corresponding calculated streamlines.	19

- 3.11 Obtained results regarding turbulence intensity infotropy for the v -velocity component (top) and for the u -velocity component (bottom), and the corresponding calculated streamlines. 20
- 3.12 Obtained results regarding the global turbulence intensity and the corresponding calculated streamlines. 21
- 3.13 Obtained results regarding the overall turbulence intensity infotropy and the corresponding calculated streamlines. 22
- A.1 Photograph of the experimental rig by Barata et al. (2008). 28

List of Tables

A.1	Principal characteristics of the Laser-Doppler Velocimeter	27
-----	--	----

List of Abbreviations and Acronyms

COV Coefficient of Variation

LDV Laser Doppler Velocimetry

pdf Probability Density Function

PSD Power Spectral Density

RMS Root Mean Square

SMI Shannon Measure of Information

V/STOL Vertical/Short Take-Off and Landing

Nomenclature

f	frequency probability or relative frequency
H	Entropy, Shannon Measure of Information, informature, infotropy [nats]
K	Constant
L	Lengthl [m]
m	Number of outcomes that form a random variable
mH	Mutual informature [nats]
N	Number of repetitions, sample size
n	Number of symbols in a message, number of classes/bins
p	Probability density
Q	Energy [J]
S	Thermodynamic entropy [J]
s	message
t	Time [s]
TI	Turbulence intensity
U	Velocity [m/s]
u	Horizontal velocity component [m/s]
V	Velocity [m/s]
v	Vertical velocity component [m/s]
W	Number of possible microstates
X, Y	Random variables, axis
x, y	Outcomes of its respective random variables X, Y
Re	Reynolds number

Greek Symbols

Δ	Interval, width [m/s], differential
δ	Variation
ν	Kinematic viscosity [m ² /s]
ϕ	Directional velocity component [m/s]
σ	Standard deviation [m/s]

Subscribed

0	Undisturbed flow
b	Logarithm base
c	Characteristic, context, convergence
I	Informational
i	Index
j	Wall jet
k	Classes
max	Maximum
n	Relative
R	Ratio
TI	Turbulence intensity

1. Introduction

After more than a century, it is safe to state that turbulence is a well-studied phenomenon but not a well-defined one. Even two decades after Lumley and Yaglom (2001) stated in their paper “A Century of Turbulence”, turbulence studies are still in their infancy (the authors mean most experiments are still exploratory) and we are still discovering how turbulence behaves in many aspects. Currently, there is an understanding of many turbulence phenomena. However, the accuracy needed for practical applications still eludes us, as nothing is approaching a comprehensive theory to fully predict and understand its behavior because turbulence’s enigmatic nature stems from its non-deterministic or stochastic characteristics.

In turbulent flows, inertial forces prevail over viscous forces, i.e., they have high values of the Reynolds number, $Re = (V_c \times L_c)/\nu$, where V_c and L_c represent a characteristic velocity and length, respectively, and ν represents the kinematic viscosity of the fluid in question. In this type of flow, some instabilities cause the formation of vortices (coherent structures in which the streamlines assume spiral-like shapes), which follow the flow with random movements, making turbulence a stochastic, non-deterministic physical phenomenon. Given the spatial location of a point in this type of flow, its instantaneous velocity oscillates around a time-averaged value. In this way, the Reynolds decomposition can be applied to the instantaneous velocity, resulting in:

$$\phi = \bar{\phi} + \phi' \quad (1.1)$$

where ϕ represents the directional velocity component, such as u in the horizontal direction, or v for the vertical direction. In Eq. (1.1), ϕ' represents the instantaneous fluctuation of the velocity around $\bar{\phi}$, which in its turn corresponds to the time-average value given by,

$$\bar{\phi} = \frac{1}{\Delta t} \int_t^{t+\Delta t} \phi dt \quad (1.2)$$

where Δt is a time interval greater than the fluctuations characteristic time.

Building on the concept of Reynolds decomposition, where the instantaneous velocity is separated into its mean and fluctuating components (Eq. (1.1)), a statistical analysis is crucial to understand the behavior of turbulent flows. In a *classic statistical treatment* of a turbulent signal, while the mean velocity (first moment), $\bar{\phi}$, provides a basic understanding of the overall flow directional trend, turbulent velocity signals often deviate from a simple Gaussian distribution due to the inherent randomness (non-determinism) introduced by the intricate vortical dynamics and interactions within the flow. The variance (second moment), denoted by σ_ϕ^2 , quantifies the intensity of these

fluctuations by representing the squared average of the velocity deviation from its mean, known as the standard deviation root-mean-square (RMS), providing a measure of the typical magnitude of these fluctuations.

While the first and second moments are valuable tools, a broader statistical description that incorporates higher-order moments, such as skewness and kurtosis, may be necessary to fully capture the complex dynamics of turbulent flows. Skewness, the third moment, can reveal the asymmetry in the distribution of velocity fluctuations, indicating a tendency for larger fluctuations in one direction compared to the other. Kurtosis, the fourth moment, describes the distribution flatness compared to a normal distribution. A higher kurtosis indicates a distribution with heavier tails trending toward a flat line, suggesting more frequent and extreme fluctuations compared to a normal distribution.

Despite the valuable insights provided by classical statistical moments, if the local turbulent velocity denotes a cluster of characteristic values leading to multimodal distributions, any analysis based on the moments is limited. For example, Silva et al. (2017) showed a renewed interpretation of oscillations of a vortex when applying finite mixtures of Gaussian distributions to capture the multimodal nature of velocity distributions. Building on our current knowledge of turbulence based on mass, momentum, and energy conservation analysis, this dissertation explores a fourth perspective rooted in *information theory*. However, it implies presenting a new lexicon associated with an *Infodynamic Analysis* aimed at providing new insights into the stochastic nature of a turbulent flowfield and assess its usefulness in an engineering context. By incorporating this new explanatory language and analytical framework, one expects to overcome the limitations of classical statistical analysis and potentially reveal deeper connections between information theoretic concepts and the complex behaviour of turbulent flows.

1.1. Objectives

Determinism and non-determinism are inherent in all physical systems. Therefore, the main objective of this dissertation is the application of an infodynamic analysis to study the informational content of physical phenomena in turbulent flows. The case study subjected to the infodynamic analysis is the flowfield beneath a V/STOL aircraft while lifting off or landing with zero or small forward momentum. The flow formed by the impact of the lift jets hitting the ground results in a wall jet that flows outward from the impingement point along the ground surface, colliding with a boundary layer flow, which generates a ground wall vortex. This phenomenon causes lift losses in the aircraft, increases the amount of air drawn in close to the ground (known as “suckdown”), in engine thrust losses following re-ingestion of the exhaust gases, and may cause aerodynamic instabilities.

With the measured data from Barata et al. (2008), this dissertation attempts to answer two questions emerging from the application of the novel lexicon of infodynamics introduced in Panão et al. (2024): How does an infodynamic perspective perform in the context of turbulence studies? What new insights can an infodynamic analysis using the new lexicon reveal about a turbulent flowfield?

The final section of this introductory chapter synthesizes how information theory

has been applied to study the amount of information in turbulent flows.

1.2. Literature Review

The literature available on turbulence is vast, but studies from the perspective of information are scarce. This forces the shortness of any literature review on turbulence infodynamics, evidencing the novelty of the informational approach explored in this dissertation. Nonetheless, this section highlights how researchers applied information theory to study turbulent flows and how far they have gone.

Turbulence is a complex phenomenon characterized by a cascade of eddies with varying length scales and corresponding oscillation frequencies, where a power spectral density (PSD) analysis offers an insightful approach to understanding the corresponding energy distribution. By decomposing the turbulent velocity fluctuations into their constituent frequencies, a PSD analysis reveals how the energy of the flow is distributed across these different frequency bands, evaluating the contribution of each one of them to the overall turbulent kinetic energy. The resulting PSD spectrum unveils a fascinating behaviour within the flow, *i.e.*, a turbulent flow begins transferring energy from the mean flow to large-scale (anisotropic) vortices. This energy then cascades down to smaller and smaller scales within the inertial subrange, eventually dissipating as heat at the Kolmogorov microscales through the process of vortex stretching. Overall, PSD analysis sheds light on the energy transfer mechanisms within turbulent flows. This information is essential for researchers studying the fundamental dynamics of turbulence, as it holds significant practical benefits in engineering applications, allowing engineers to assess turbulence intensity and design structures and systems that can withstand turbulent forces.

Previous works were conducted by Cerbus (2014) in his Ph.D. thesis, whose intention, in the spirit of pure mathematics, was to use information theory (prior to the new lexicon) and its close relative computational mechanics in the study of turbulence. He devoted his attention primarily to the examination of two-dimensional turbulence, specifically delving into (what he has called) an *information-theoretic treatment* of general eddy energy cascade ideas and the deviations from their simple predictions, known as the study of intermittency. At that time, applying information theory to a physical system was like navigating without a compass, and thus by directly incorporating its concepts, Cerbus (2014) organized velocity measurements into partitions and used them to produce the relative frequencies used to determine informational quantities and identify problems regarding it. This process is on par with the *infosensors* concept brought by the new lexicon, and despite not using the same “calibration” explored in Chapter 2, his findings point in a similar direction. Moreover, it emphasizes an important aspect of this field: guiding the engineer in asking the right questions.

Cerbus (2014) concluded that when the Reynolds number is sufficiently large for the flow to develop a cascade, the flow behaviour becomes dependent on Reynolds (Re) in the sense that spatial features of turbulence behave in a manner not previously considered. Namely, he found that the flow unpredictability decreases with increasing Re . Furthermore, his information-theoretic treatment of turbulence revealed the existence of a second transition in turbulence, where “structureless” fluctuations become cascade turbulence.

Building upon Cerbus (2014)'s work, Abbaszadeh et al. (2021) explored waterborne chemical plumes as a model for molecular communication in a macroscopic system. They applied and interpreted concepts from fluid turbulence theory within the context of molecular communication to characterize an information cascade. This work exemplified the application of information-theoretic principles to real physical systems, moving beyond the purely mathematical perspective of Cerbus (2014). Their findings corroborated those of Cerbus (2014), demonstrating that the information dissipation rate decreases with increased turbulence levels (higher Reynolds numbers) due to more efficient mixing, weakening the remaining power of the molecular signal.

Lozano-Durán and Arranz (2022) goal was to further advance the field of turbulence research by assessing the problems of causality, modelling, and control for chaotic, high-dimensional dynamical systems, formulated in the language of information theory. One intriguing conclusion between their conclusions regards the reduced-order modelling of chaotic systems, which has been posed as a problem of conservation of information: modelled systems contain a smaller number of degrees of freedom than the original system, which in turn entails a loss of information. Thus, the primary goal of modelling is to preserve the maximum amount of useful information from the original system. They have derived the conditions for maximum information-preserving models and shown that accurate models must maximize the mutual information between the model state and the true state, and minimize the Kullback-Leibler divergence between their probabilities, *i.e.*, the difference between the system's maximum amount of information for the number of possible categories and the actual amount of information. The mutual information assists the model in reproducing the dynamics of the original system, while the Kullback-Leibler divergence enables the accurate prediction of the statistical quantities of interest.

Despite reaching notable conclusions, Abbaszadeh et al. (2021) and Lozano-Durán and Arranz (2022) directly used the system's probability density function to determine its informational content. In contrast to them, Granero-Belinchón et al. (2018) uses a nearest neighbour estimator described by Leonenko et al. (2008) to determine the probabilities and accurately compute the informational contents from an experimental time series. Their paper analyzed multifractality and intermittency related to the deformation of a probability density function from Gaussian at large scales to non-Gaussian at smaller scales of turbulence. None of these works expresses their application of information theory as an infodynamic analysis, and only Cerbus (2014) touches on the topic of determining the probabilities that characterize the physical system under study. Therefore, the next chapter aims to introduce this new perspective based on quantifying the amount of information in a stochastic physical system.

2. Infodynamic Analysis Fundamentals

Following Panão et al. (2024), infodynamics is a perspective on how information behaves and changes within a system while developing. An infodynamic analysis examines the behavior and evolution of informational content within a physical system over time. It uses a novel lexicon introduced in Panão et al. (2024) with new terms such as *informature*, *infotropy*, and *infosensor*, which quantify and encapsulate the non-deterministic or/and stochastic nature on any physical system. Even though these concepts are rooted in statistics, both fields are not competitive. Thus, an infodynamic analysis applied to turbulence aims to offer a different perspective in an attempt to unravel its longstanding conundrum: randomness.

2.1. New Lexicon of Infodynamics

The concept of information as a quantifiable variable was introduced by Claude Shannon (1948) in his 1948 seminal work on “A Mathematical Theory of Communication” through the formulation of H (see Eq. (2.1)), a measure of the amount of information in a message based on its statistical analysis. Shannon described it as “*measure of information, choice, and uncertainty*”.

$$H = -K \sum_{i=1}^m f_i \log_2(f_i) \quad (2.1)$$

Shannon understood a message s as a sequence of n symbols described by a random variable X , which consists of a set of m different possible outcomes and their frequency probabilities f_i forming the probability distribution $f(X)$, with $\sum_i f_i = 1$. Eq. (2.1) represents the most elementary form of H , to which K is more than an arbitrary constant, as argued in Tribus and McIrvine (1971), but a contextual scale.

At the outset, the probability distribution describing a physical system is not known, justifying the reason for using a frequency probabilistic approach to statistically describe the system. In this scenario, each symbol in a message, s_i , corresponds to a physically measured value (see Fig. 2.1). Its frequency probability or relative frequency is determined by counting the number of occurrences of each symbol in s and dividing it by the total number of symbols in the message.

In his work, Shannon assigned the symbol H to represent entropy, which, according to Tribus and McIrvine (1971), was influenced by a comment from John Von Neumann because of its resemblance to the formulation already established for thermodynamic entropy. However, Denbigh (1981) argued that this was a disservice to Shannon’s work

$$\begin{array}{l}
 \mathbf{S} = \{ s_1, s_2, s_3, s_4, s_5, s_6, \dots, s_n \} \\
 \curvearrowright \\
 X = \begin{cases} x_1, & \text{if the outcome is ...} \\ \dots & \dots \\ x_m, & \text{if the outcome is ...} \end{cases}
 \end{array}$$

Figure 2.1: Schematics of the message s and the random variable X that defines it.

because functions with the same formal structure do not necessarily represent the same concept. Despite the latest argumentation coming from Ben-Naim (2017), suggesting the correct term would be *Shannon Measure of Information* (SMI), this dissertation follows the different lexicon presented in Panão et al. (2024), which is simpler and useful to engineering practice. This lexicon implies the identification of distinct elements in Shannon’s formulation through a detailed analysis of the contextual scale K and the units of information, resulting in three neologisms: *informature*, *infotropy*, and *infosensor*.

2.1.1. Informature

Informature is the block in Shannon’s formulation that quantifies the information content from the knowledge of the frequency probability distribution characterizing a physical system regardless of its context:

$$H_{I,b} = -K_b \sum_{i=1}^m f_i \log_2(f_i) \quad (2.2)$$

where K_b is the second part of $K = K_c \cdot K_b$ in Eq. (2.1) and is responsible for the units of information by establishing the logarithm base. Turbulence’s non-deterministic nature has its informational content maximized by a Gaussian distribution, where its statistical perspective is given by a mean velocity and by its variance. Thus, its units should be in “natural units” abbreviated as *nats*, accounted by the logarithm base changing to the natural logarithm when $K_b = \ln(2)$, with $b = e$. If the message were to be binarized, then the logarithm should be in the original base-2 of Shannon’s formulation, $K_b = \log_2(2) = 1$, and *informature* would be in “binary units” or *bits*, with $b = 2$.

Contrasting deterministic systems, where initial conditions determine future states and make them predictable, turbulence displays stochasticity and complex dynamics. *Informature* offers valuable insights into its non-deterministic nature by capturing its variability and diversity, and thus, by quantifying its informational content, bringing new insights regarding the behavior governing underlying dynamic mechanisms structuring the flow, helping to detect emergent patterns, and identifying subtle variations that may denote significant changes.

2.1.2. Infotropy

As mentioned in Section 2.1, John Von Neumann suggested the name entropy because of Eq. (2.1) resemblance to the thermodynamic entropy. However, do thermo-

dynamic entropy and Shannon entropy truly represent the same concept, or are they at least related? In the field of the theory of gases, when considering the presence of W molecules, the system would present W possible microstates with the same probability of existing, thus being represented by a uniform probability distribution, $f_i = 1/W$. Applying this to Eq. (2.2), this system's *informature* in natural units results in

$$H_{I,e}^W = - \sum_{i=1}^W \frac{1}{W} \ln \left(\frac{1}{W} \right) = \ln(W) \sum_{i=1}^W \frac{1}{W} = \ln(W) \quad (2.3)$$

This result by itself merely expresses that the average degree of surprisal in the outcome is directly related to the number of microstates. However, when using the Boltzmann's constant, k_B , as the contextualized part (K_c) of the contextual scale K in Eq. (2.1), given by the ratio between the gas constant, R_0 , and Avogadro's number, N_A , the classical thermodynamic entropy, S , emerges as a contextualized informature:

$$H_e^W = k_B \cdot H_{I,e}^W = k_B \cdot \ln(W) = S \quad (2.4)$$

The solution for the classical debate on the physical meaning behind thermodynamic entropy is to understand that it is a measure of possibility among the several W microstates rather than a measure of disorder. This can now be linked with Clausius's macrostate invention of the word *entropy* to Boltzmann's microstate interpretation: $\delta Q = T \cdot S$, where δQ is the energetic "price" paid for the existence of W possible configurations of the gas molecules at a certain reference temperature. Therefore, a contextualized *informature* allows measuring the degree of transformation of a physical system due to its non-deterministic nature through the quantification of the amount of information one needs to learn anything about it. This measurement is referred to as *infotropy*, and it is generally given by:

$$H_b = K_c \cdot H_{I,b} \quad (2.5)$$

with K_c as the first part of the K contextual scale parameter in the original Shannon's formula Eq. (2.1). However, special attention should be given to the infodynamic simultaneous measure of two (or more) distinct characteristics of a system.

2.1.3. Mutual Informature

Given two messages, one described by the random variable X and the other by the random variable Y , the *mutual informature*, $mH_{I,b}(X, Y)$, is the measure of information shared between these variables as illustrated in Fig. 2.2.

It is often interpreted as the average reduction in uncertainty in one message when the other message is known, or how the variability and diversity of one variable affects the other and vice versa:

$$mH_{I,b}(X, Y) = H_{I,b}(X) + H_{I,b}(Y) - H_{I,b}(X, Y) \quad (2.6)$$

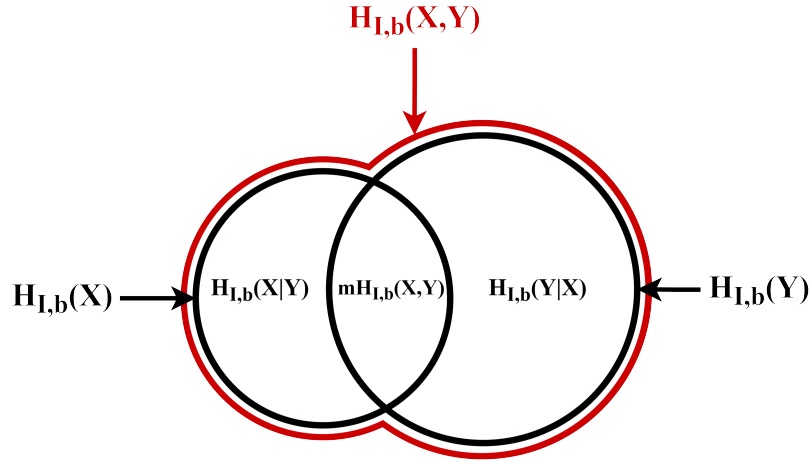


Figure 2.2: Venn diagram of *mutual informature* between two messages, one described by the random variable X and the other by the random variable Y , interpreted from Stone (2015).

In Eq. (2.6), $H_{I,b}(X, Y)$ is the *joint informature* given by the random variables' joint probability distribution, $f(X, Y)$, representing the total informational content between both messages:

$$H_{I,b}(X, Y) = K_b \cdot \sum_{i=1}^{m_x} \sum_{j=1}^{m_y} \left[f(x_i, y_j) \cdot \log_2 \left(\frac{1}{f(x_i, y_j)} \right) \right] \quad (2.7)$$

In the case of independence between both messages, probability laws express $f(X, Y) = f(X) \cdot f(Y)$, which in turn makes $H_{I,b}(X, Y) = H_{I,b}(X) + H_{I,b}(Y)$, implying that $mH_{I,b}(X, Y) = 0$. When the *mutual informature* is zero, it indicates independence between the relevant random variables. In simpler terms, this suggests that there is no relationship between the two messages. When X and Y coincide, the mutual informature is maximum resulting in $H_{I,b}(X, Y) = 0$ and $mH_{max,b} = H_{max,b}(X) + H_{max,b}(Y)$. Implementing Eq. (2.7) and Eq. (2.2) in Eq. (2.6), the *mutual informature* can be directly obtained by:

$$mH_{I,b}(X, Y) = K_b \cdot \sum_{i=1}^{m_x} \sum_{j=1}^{m_y} \left[f(x_i, y_j) \cdot \log_2 \left(\frac{f(x_i, y_j)}{f(x_i) \cdot f(y_j)} \right) \right] \quad (2.8)$$

2.2. Calibrating Infosensors

In the field of infodynamic measurement science, as explained in Panão et al. (2024), an *infosensor* is an instrument or measurement technique that captures the non-deterministic nature inherent in a physical system. It measures the different possibilities for a certain characteristic, and through statistics obtains the relative frequency distribution of values that measure *informature* or the amount of information one needs to learn something about the physical system.

Putting into perspective, when using a ruler to measure length or a scale to measure mass, the equipment involved in these processes needs to be calibrated. For example,

the pre-established SI reference distance is used for calibration in the case of rulers, while piezoelectric sensors are used to convert the electrical charge generated by certain materials when subjected to mechanical stress into a calibrated mass value. Similarly, in the field of infodynamics, an infosensor also requires calibration in order to measure *informature*.

The formulation in Eq. (2.2) implies its applicability in the discrete domain. However, a turbulence velocity is a random variable existing in the continuous domain. As expressed by Stone (2015), unlike other cases where the results obtained by discrete variables can be extended to continuous variables, since *informature* is an extensive property depending on the system's size, the change from the discrete to the continuous domain requires a careful analysis.

Continuous random variables are described by a probability density function (pdf) instead of a frequency probability distribution, which implies that a histogram for the random variable X in the discrete domain containing classes with a finite width, Δx , approaches the continuous domain if $\Delta x \rightarrow 0$. This change eventually leads to an infinite number of classes or bins, n_k . This is quite problematic, given that *informature* is an extensive property and depends on the number of classes defined for the available data, *a priori* one does not know how much data one needs to stabilize the distribution of values. Consequently, with an increasingly larger data sample, and enough data resolution to allow decreasing the size of histogram classes approaching the continuum, the *informature* tends to infinity. This can be proved by considering the probability density, p_i ,

$$p_i = \frac{f_i}{\Delta x} \Leftrightarrow f_i = p_i \cdot \Delta x \quad (2.9)$$

and replacing Eq. (2.9) in Eq. (2.2):

$$\begin{aligned} H_{I,b} &= - \sum_{i=1}^{n_k} p_i \Delta x_i \log_b(p_i \cdot \Delta x_i) \\ &= - \sum_{i=1}^{n_k} p_i \Delta x_i \log_b(p_i) + \sum_{i=1}^{n_k} p_i \Delta x_i \log_b\left(\frac{1}{\Delta x_i}\right) \\ &= - \sum_{i=1}^{n_k} p_i \Delta x_i \log_b(p_i) + \log_b\left(\frac{1}{\Delta x_i}\right) \\ &\stackrel{\Delta x_i \rightarrow 0}{=} - \int_{-\infty}^{\infty} p_i \log_b(p_i) dx + \infty \end{aligned} \quad (2.10)$$

Eq. (2.10) reveals an intriguing observation: all continuous variables exhibit infinite *informature*. This suggests that drastically different distributions can possess the same (infinite) *informature*, as expected from extensive properties when their size domain approaches infinite. However, the first term in Eq. (2.10) corresponding to a *differential informature*, $H_{\Delta,b}$, is always finite and reveals an interpretation of *informature* as an intensive informational property of the system that no longer depends on the number of classes/bins, n_k .

$$H_{\Delta,b} = k_b \cdot \sum_{i=1}^{n_k} f_{\Delta,i} \log_2(p_{\Delta,i}) \quad (2.11)$$

Moreover, it is possible to obtain analytical solutions of $H_{\Delta,b}$ for several mathematical probability density functions, offering a direct comparison between these functions and the histograms produced from data to assess whether or not the function describes data. It is not a goodness-to-fit test, but an informational fitting test.

To better illustrate these concepts, for the velocity measured from the LDV signal in one point (later explained in Section 3.1), one applies the rule defined by Bendat and Piersol (1966) for determining the number of classes based on the sample size,

$$n_k = 1.87 \cdot (N - 1)^{2/5} \quad (2.12)$$

Fig. 2.3 illustrates the *informature*'s growth with the number of classes, while the *differential informature* stabilizes after, approximately, $N_c = 1000$ data samples, to which according to the time vector provided by the LDV, corresponds to a system's response time of 22 seconds.

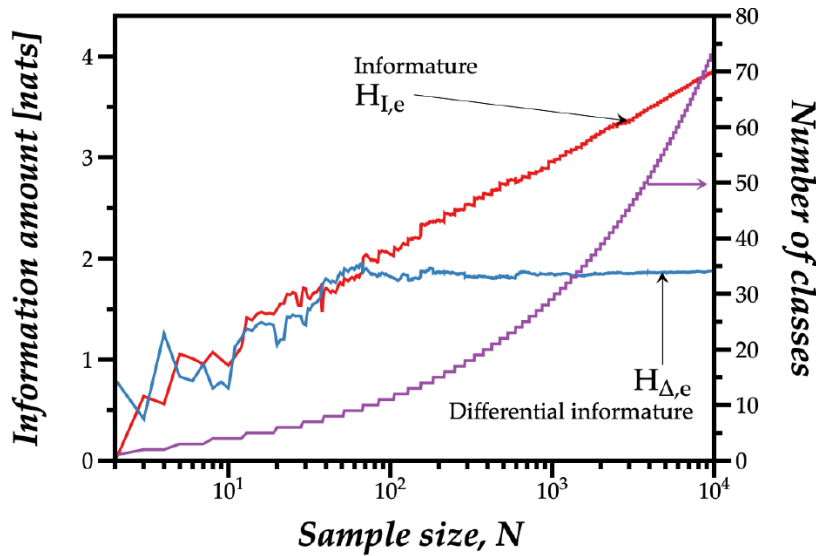


Figure 2.3: Evolution of *informature*, $H_{I,e}$, *differential informature*, $H_{\Delta,e}$, and the number of classes with the growth of the data sample size, N , by Panão (2024).

If the number of classes is fixed by a sample size greater than the *differential informature*'s convergence sample size, N_c , then the value of *informature* eventually stabilizes, indicating that *informature*'s calibration has been performed. Additionally, by dividing the calibrated *informature* by its maximum value, $H_{max,b} = \log_b(n_k)$, where all the classes n_k have the same number of samples inside, another way of converting *informature* from an extensive to an intensive property is obtained: the *relative informature*, H_n .

$$H_n = \frac{H_{I,b}}{H_{max,b}} \quad (2.13)$$

Relative informature's value ranges from 0 to 1, indicating the level of indeterminacy in the system. A value of 0 represents a fully regular system with no indeterminacy and a single value repeated N times. In contrast, a value of 1 represents a fully indeterminate system with the same sample size for each unique measured value.

The next chapter applies these infodynamic concepts to the turbulent flow generated by a ground vortex using data from Barata et al. (2008).

3. Infodynamic Analysis of Turbulence in Ground Vortex

The wall jet interaction with the boundary layer free stream results in the formation of a highly curved flow (ground vortex) far upstream of the impinging jet, which has profound influences on flow development. To further investigate this phenomenon, Barata et al. (2008) designed an experimental method in which a wall jet interacts with a wind tunnel's produced boundary layer, creating a highly curved region. Their goal was to identify the parameters, relevant regimes, and structures associated with instabilities, and other secondary effects of a ground vortex flow.

LDV measurements of a two-component velocity field were the input values used in this dissertation to apply the novel infodynamics lexicon and take a step forward in the continuous attempt to understand the non-deterministic nature and impact of turbulence in engineering.

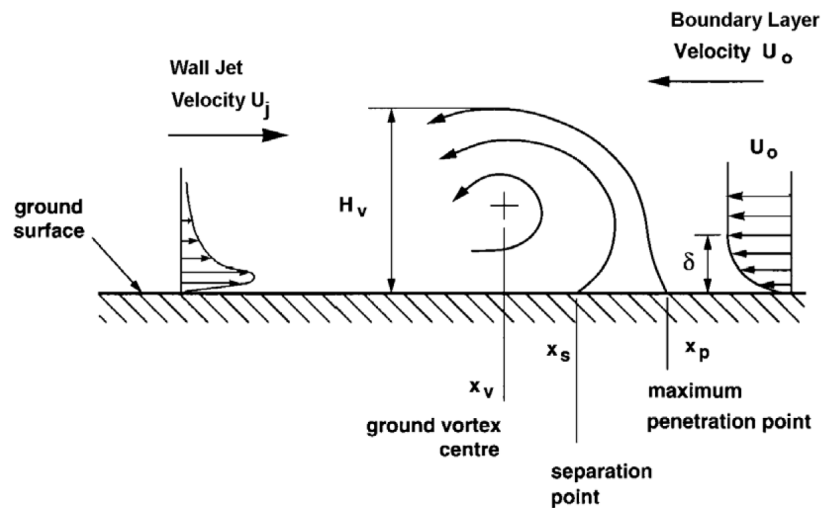


Figure 3.1: Diagram of the ground vortex facility by Barata et al. (2008).

3.1. Ground Vortex Velocity Characterization

The collision between the wall jet and the boundary layer results in an upwards-curved flow. The measured and observed data by Barata et al. (2008) has shown that this flow field contains the presence of three distinct main turbulent structures: a ground vortex, a small vortex, and a secondary vortex. These structures are depicted in Fig. 3.2.

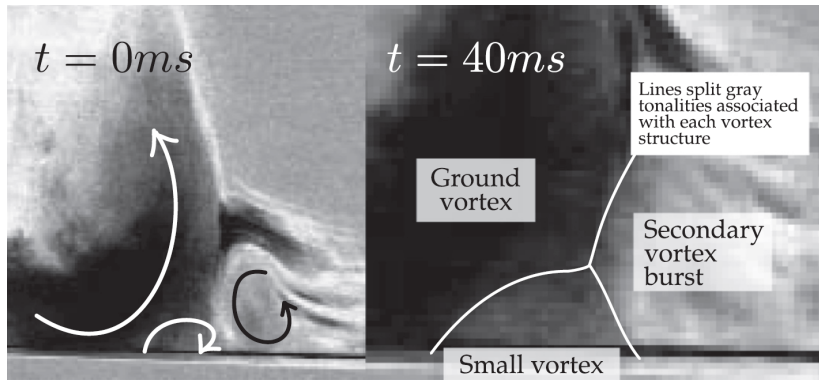


Figure 3.2: Illustration of the three vortical rotation directions (ground vortex, secondary and small vortices). Detail of the intersection region where different tonalities in grey allow distinguishing the three vortices by Silva et al. (2017).

As Barata et al. (2008) explains, in addition to the upwards-curved flow resulting from the collision between the wall jet and the boundary layer upstream of the separation point and before the maximum penetration point, the flow inside the boundary layer has a downward movement toward the ground, forming the anticlockwise vortex associated to the secondary vortex. This anticlockwise vortex then merges with a small one that is growing between the main ground vortex and the secondary vortex. As the resulting vortex continues to grow, it exceeds the boundary layer's height and suddenly breaks, being carried upwards in the direction of the curved flow.

In order to gain a better understanding of these phenomena, Barata et al. (2008) performed an experimental visualization study and Fig. 3.3 depicts the behavior of the secondary vortex. It is noteworthy that Fig. 3.3 corresponds to a wall jet-to-crossflow velocity ratio of $U_R = 1.74$, which demonstrates similar characteristics to the evaluated data in this thesis for $U_R = 2$.

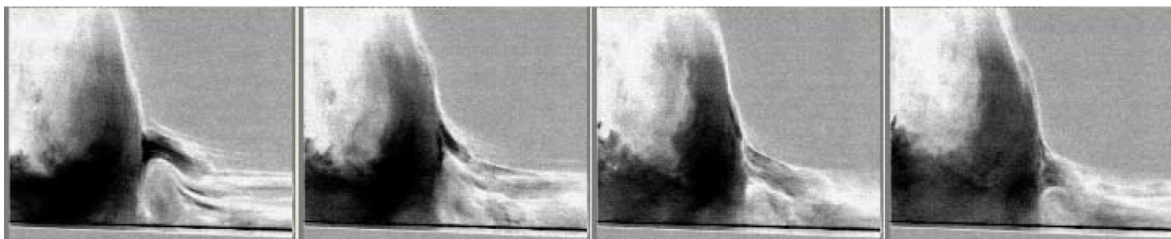


Figure 3.3: Small vortex burst and new vortex growth for $U_R = 1.74$. Frames instants: $t=0s$; $1/25s$; $2/25s$; $3/25s$. Figure taken from Barata et al. (2008).

The mapping of the turbulent flow velocity field made at the vertical plane of symmetry for a wall jet mean velocity of 13.7 m/s and mean boundary layer velocity of 6.9 m/s corresponded to a wall jet-to-crossflow velocity ratio of $U_R = U_j/U_0 = 2$ (Barata et al., 2008). Considering the height of the tunnel as the characteristic dimension, the Reynolds numbers for the boundary layer and wall jet are 1.4×10^6 and 1.4×10^4 , respectively. A brief overview of the experimental setup is provided in Chapter A. However, for data processing orientation purposes, the origin of the horizontal, X , and vertical, Y , is taken near the maximum penetration point. The X coordinate is positive in the wall jet flow direction, and Y is positive upwards.

Evaluating the calculated mean velocities portrayed in Fig. 3.4, and superimposing the streamlines reported in Barata et al. (2008), the mean velocity maps confirm the conditions for the emergence of an unstable secondary vortex considering the negative value of vertical velocity component near the ground in the region delimited by $0 < y \text{ [mm]} \leq 30$ and $x < 0$ mm, and its positive value elsewhere, confirming that its center is located downstream ($X > 0$) of the separation point (see Fig. 3.1), but probably somewhere before the maximum penetration point. Also, the mean velocity maps appear unable to provide a location for the ground vortex center (illustrated in Fig. 3.1) from the zero values of the horizontal velocity component or the maximum values of the vertical velocity component because these do not coincide: the maximum vertical velocity component occurs at $x = -40$ mm and $y = 120$ mm, only slightly displaced in the crossflow direction, and the minimum horizontal velocity component occurs also at $y = 120$ mm, but $x = -120$ mm. However, the RMS velocity contains some insights regarding the location of the vortex center.

Fig. 3.5 depicts the map of the fluctuation mean velocity integrated over time. Both the horizontal and vertical velocity component maps reveal a high fluctuation associated with the epicenter of the ground vortex (bright yellow zone) at the same location. However, since this parameter is a time-integrated measure, there are no signs of the presence of any secondary vortex. This indicates that its detachment and subsequent convection by the upward-curved flow occurs in a small fraction of time (relative to the total measurement time) that is not enough to capture its occurrence in these average maps.

Additionally, regarding the mean velocities, Silva et al. (2017) approached the characterization of the velocity in terms of characteristic velocity values capturing multiple clusters of velocity distribution with similar features through finite mixtures. Therefore, in the case of the measured bimodal distributions, Silva et al. (2017) retrieved positive characteristic velocities in the horizontal direction in the region $-120 < x \text{ [mm]} < 20$, while negative characteristic values in $-40 < x \text{ [mm]} < 120$. This mixture of Gaussian distributions indicates the effects of the wall jet could extend to $x = 20$ mm downstream of the separation point, while the influence of the boundary layer still persists until $x = -40$ mm upstream of the separation point. This implies that the interaction between the wall jet and the boundary layer occurs within the region between $x = -40$ mm and $x = 20$ mm.

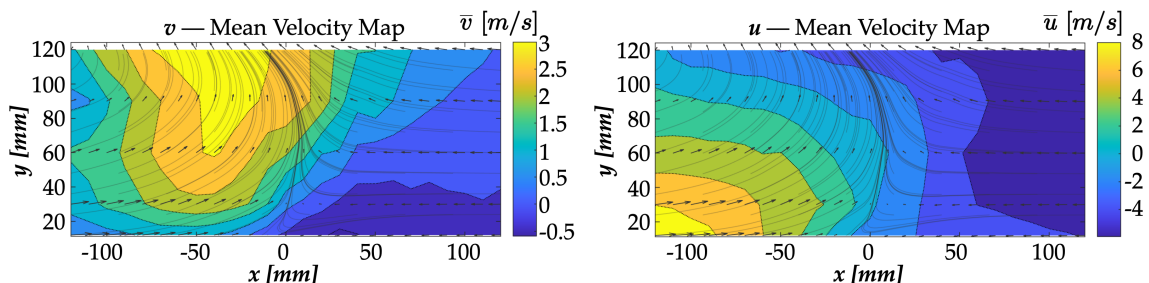


Figure 3.4: Map of mean velocity regarding the vertical component, \bar{v} (left) and horizontal component, \bar{u} (right) superimposed with the corresponding streamlines from Barata et al. (2008).

The parameters analyzed in Figures 3.4 and 3.5, while commonly used in statistical studies of turbulence, offer a limited view of the flow field. These maps only capture

basic turbulent characteristics of the flow field under analysis, such as the presence of the ground vortex, the possibility of the secondary vortex, and the streamlines confluence boundary associated with the upward-curved flow resulting from the interfacial converging lines depicting the collision between the wall jet and the boundary layer. However, these parameters are not sensitive enough to the full spectrum of turbulent phenomena within the system.

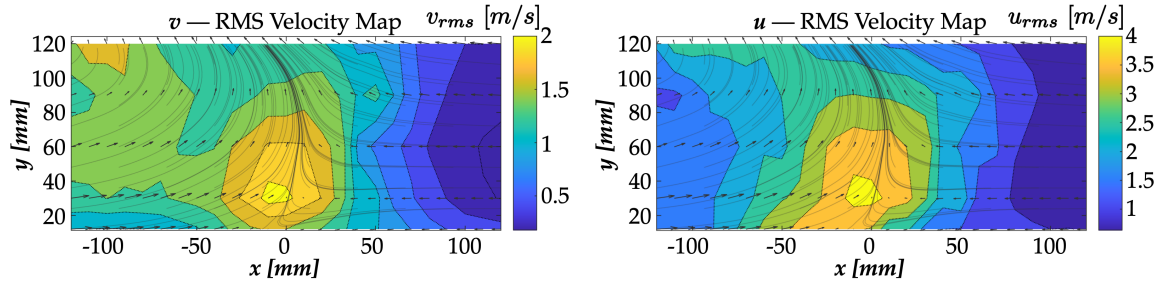


Figure 3.5: Map of the average velocity fluctuations regarding the vertical component, v_{rms} (left) and horizontal component, u_{rms} (right) superimposed with the corresponding streamlines from Barata et al. (2008).

3.2. Informature Maps of Velocity fields

The data provided by the LDV velocity signals consider 25 locations in the flow field at Y [mm] = [12; 30; 60; 90; 120] and X ranging from -120 mm to 120 mm with increments of 10 mm. Each measurement point contained a sample of 10000 measurements of both the horizontal, u , and vertical, v , velocity components. For an adequate calibration of the LDV system as an infosensor, the data sample size implies defining 74 velocity classes (n_k) for the infodynamic treatment of each signal based on Bendat and Piersol (1966) rule in Eq. (2.12). All velocity component signals were calibrated to the same size class, and edge values of all classes were enclosed between the lowest and highest measured values for each velocity component. According to Fig. 3.6, the *infosensor* calibration was a success, as the *informature* values converged.

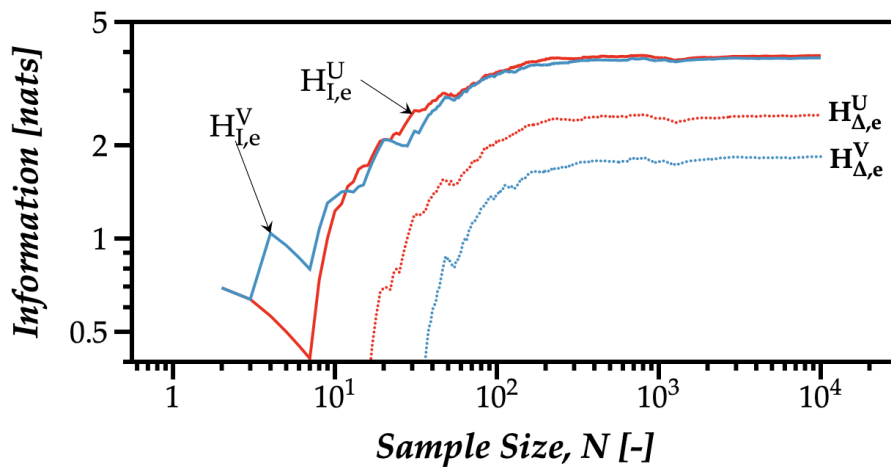


Figure 3.6: Example of the evolution of the *informature*, $H_{I,e}$, and *differential informature*, $H_{\Delta,e}$, relative to the velocity component u , v , as the data sample size (N) grows. This case corresponded to the LDV signal point for $Y = 60$ mm and $X = 0$ mm.

The *Informature* maps for both velocity components shown in Fig. 3.7 distinguish the informational value obtained from each component. Namely, while the vertical velocity component captures the ground vortex epicenter (similar bright yellow), also identified in the v and u RMS maps, in the horizontal velocity component case, a region of a high amount of information becomes clear. This area is immediately before the stagnation boundary, indicating complex dynamics starting at the bottom and dragging upwards. It is a signature that one could attribute to the small secondary vortex that grows and develops until detachment, followed by its upward convection by the main ground vortex. Another noteworthy observation in both maps is the low *informature* values in the downstream region of the stagnation boundary, as expected due to the presence of the relatively uniform undisturbed flow. In contrast to the maps in Figures 3.4 and 3.5, the *informature* maps reveal a more faithful view of the structures that induce diversity to the flow field.

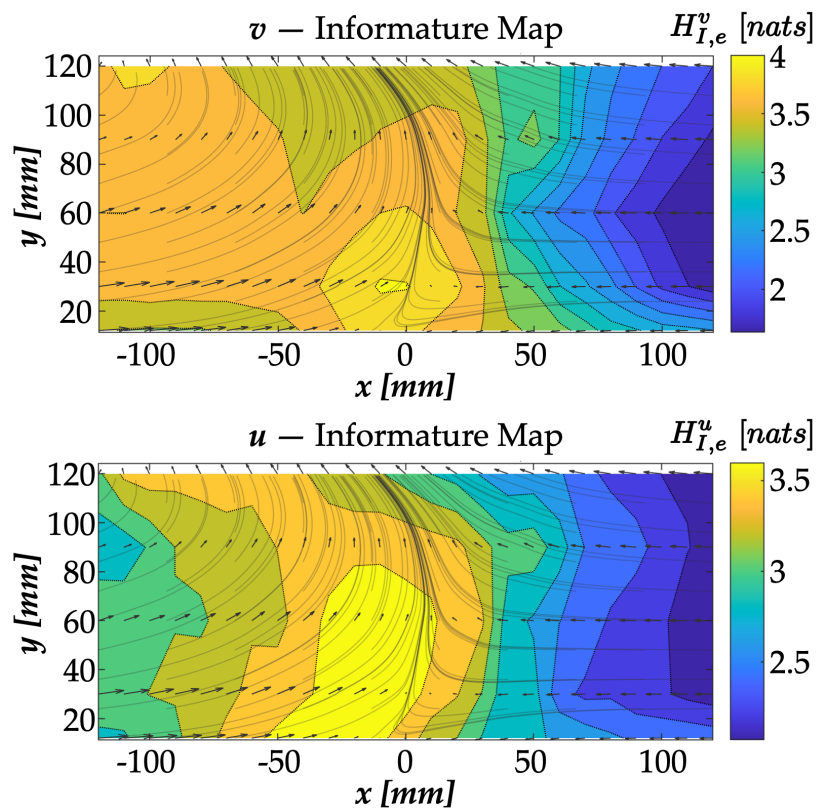


Figure 3.7: Obtained *informature* map regarding the v -velocity component (top) u -velocity component (bottom) and the corresponding calculated streamlines.

Fig. 3.8 illustrates a case where the *mutual informature* value does not converge due to the non-stabilization of the v -velocity component's *informature* compared to the u -velocity component, and thus it emphasizes the calibration value of the infosensor. Therefore, for the aforementioned successful calibration, the *mutual informature* map in Fig. 3.9 exhibits sufficiently high values, via two high informational regions crossing the boundary defined by the streamlines confluence, allowing to conclude that both velocity components are related, particularly in those regions. This highlights the importance of measuring simultaneously both velocity components in this type of study, as they are not independent.

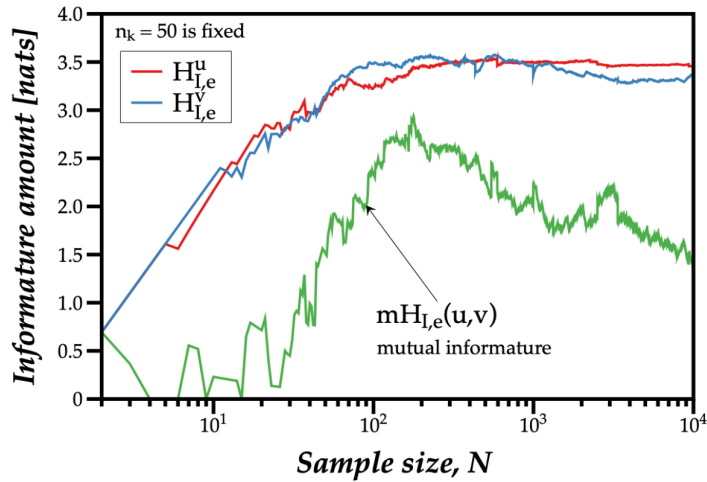


Figure 3.8: Evolution of the *informature*, $H_{I,e}$, relative to the velocity component u , v , and the *mutual informature*, $mH_{I,e}(u,v)$, as the data sample size, N , grows, by Panão (2024).

One of the possible meanings for a high u, v *mutual informature* is the indication of coherent structures associated with substantial changes in the flow. The region surrounding the peak on the upstream side of the confluence line and the region on the upper part of the downstream side are regions where one expects higher momentum transfer from the original direction of each flow (jet and boundary layer) and the new direction defined by the resulting ground vortex. Such intense momentum exchanges point to stronger correlations between the u and v velocity components of the flow captured by the *mutual informature* map plotted from infodynamic measurements of the raw data.

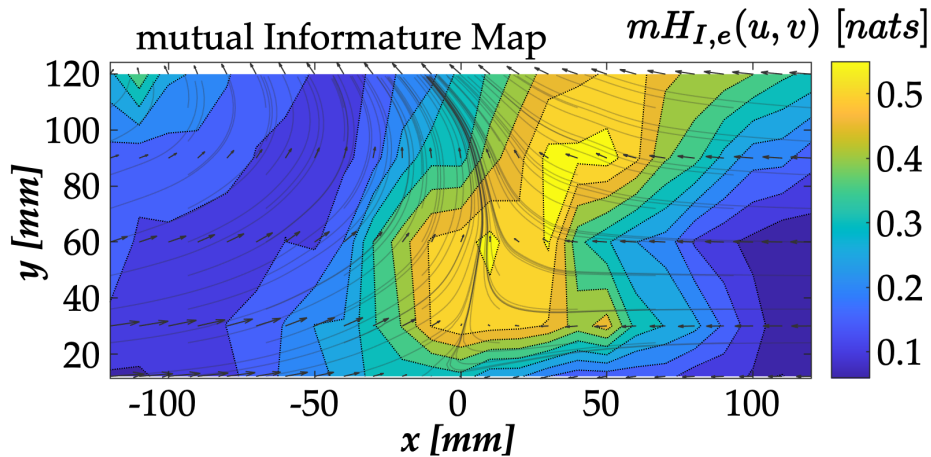


Figure 3.9: *Mutual informature* map between the horizontal, u , and vertical, v , velocity components.

The last section considers a possible infodynamic insight related to the turbulence intensity assessment, especially when the average velocity is low and close to stagnation.

3.3. Turbulence Intensity Infotropy

Turbulence Intensity (TI) measures the degree of disturbance in a flow. Understanding the levels of turbulence intensity has significant implications across various

fields. In aeronautics, the drag on an airfoil is related to TI , directly affecting fuel efficiency and, in extreme cases, aircraft stability (Yap et al., 2001). Similarly, in the automobile industry, TI measurements are crucial for evaluating the aerodynamics of auto body designs (Passaggia et al., 2021). In chemical processes, high TI can be beneficial for promoting intentional mixing. Still, it can also be detrimental, as excessive TI at the face of a chemical fume hood may lead to unwanted spillage of chemical fumes into a laboratory (Tseng et al., 2010). These examples underscore the diverse and critical roles that turbulence intensity plays in engineering, safety, efficiency, and comfort across various industries. Its definition is equivalent to the statistical parameter, Coefficient Of Variation (COV), using the mean of the velocity fluctuation as the parameter expressing the “variation” and comparing it to the mean velocity of the flow. Assuming an isotropic turbulent flow, the turbulence intensity of the u -velocity component would be

$$TI_u = \frac{\sqrt{\overline{u'^2}}}{\overline{|u|}} \quad (3.1)$$

with $\overline{|u|}$ as the mean of the absolute velocity in the x direction. The velocity v would have a similar formulation. The reason for considering the absolute value of each velocity is to avoid the canceling effect on the average exerted by velocity values in opposite directions. Fig. 3.10 presents the TI maps for the vertical (v on the left) and horizontal (u on the right) velocity components superimposed with the average velocity streamlines, similarly to previous maps.

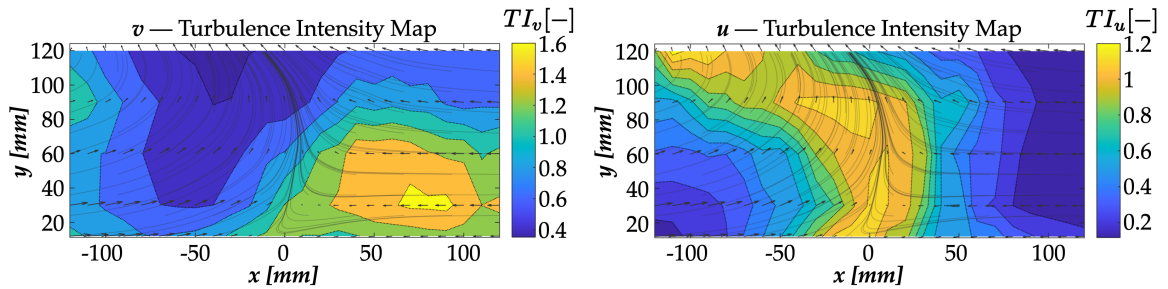


Figure 3.10: Obtained results regarding turbulence intensity for the v -velocity component (left) and for the u -velocity component (right), and the corresponding calculated streamlines.

The v -velocity component turbulence intensity map (TI_v) depicted in Fig. 3.10 (left) shows high TI values where the boundary layer has low mean velocity because it is the boundary layer flow region less affected, on average, by the momentum exchanges induced by the ground vortex. The u -velocity component turbulence intensity TI_u evidences a higher turbulence region departing from the stagnation region. This region of high TI_u values appears compatible with a mixed effect of the interaction line between the ground vortex and the boundary layer and the “trajectory” of the formation and detachment of the small vortex close to the stagnation point. While the mapping of TI_u is insightful, the TI_v contains the challenge of evaluating turbulence intensity in regions of low mean velocity, where the limit is obtaining a turbulence intensity value approaching infinite. To overcome this turbulence intensity limitation, this dissertation explores the *infotropy* concept described in section 2.1.2, using the turbulence intensity to contextualize the *informature*. However, to keep the result dimensionless, one uses the *normalized informature* defined in Eq. (2.13). The *normal-*

3. Infodynamic Analysis of Turbulence in Ground Vortex

ized *infotropy* is a measure of diversity in a system, allowing a good representation of the system's non-deterministic variability. Therefore, using the classic turbulence intensity as a contextual scale, $K_c = TI$, Eq. (2.5) results in a *turbulence intensity relative infotropy*, $H_{e,TI}$, defined as

$$H_{e,TI}^{veloc} = TI_{veloc} \cdot H_n \quad (3.2)$$

Fig. 3.11 depicts the *infotropy* results for the v (top) and u (bottom) velocity components. While the $H_{e,TI}^u$ maintains the insight already provided by the TI_u map, the vertical TI *relative infotropy* map now shows higher values in the region where ground vortex, secondary vortex, and small vortex converge, revealing a high degree of informational transformation, and providing meaningful insights on the contribution of the vertical velocity component turbulence intensity to the turbulent flow development. Thus, it overcomes the shortcomings of low mean velocity values. It would be interesting to apply this infodynamic approach to other boundary layer flows near the wall to evaluate further its explanatory potential.

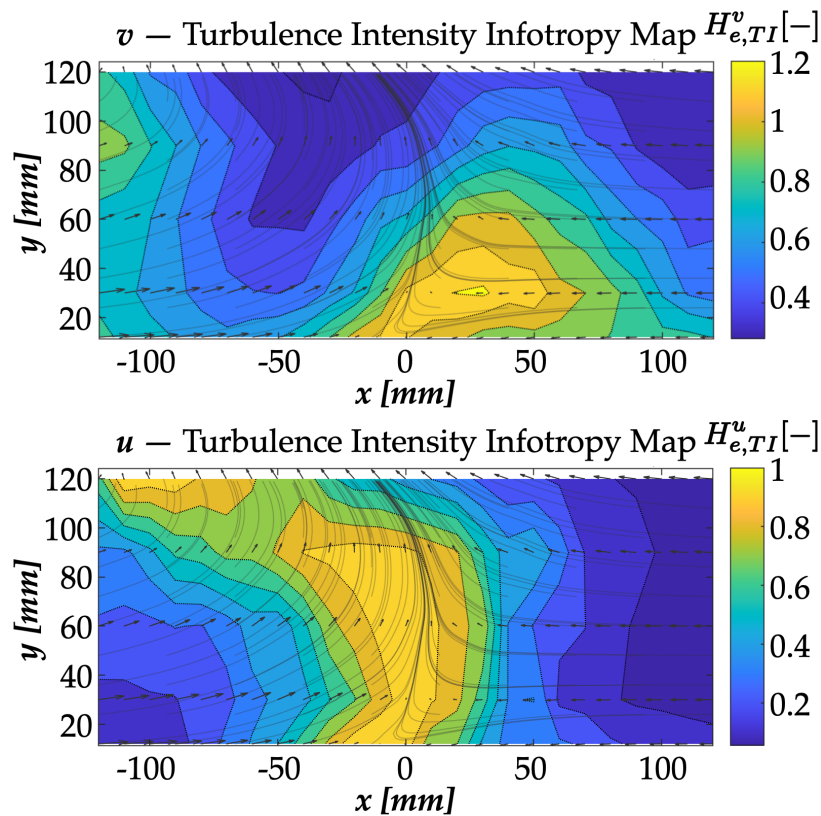


Figure 3.11: Obtained results regarding turbulence intensity infotropy for the v -velocity component (top) and for the u -velocity component (bottom), and the corresponding calculated streamlines.

The maps analyzed for each velocity direction provide directional insight into the anisotropic character of this turbulent flow. However, one can also perform a combined analysis of turbulence intensity using both velocity components to capture an overall turbulence level. Considering the experimental setup of Barata et al. (2008) (see also A), the experimentally simulated turbulent flow was essentially 2D. Therefore, one

neglects a third velocity component. In this sense, the overall mean velocity in each location with N data samples available corresponds to

$$\bar{U} = \frac{1}{N} \sum_{i=1}^N \sqrt{u_i^2 + v_i^2} \quad (3.3)$$

Then, the overall velocity fluctuation of each measurement i would be $U'_i = \sqrt{u_i^2 + v_i^2} - \bar{U}$, implying an overall RMS of

$$U_{\text{RMS}} = \sqrt{\frac{1}{N} \sum_{i=1}^N (U'_i)^2} \quad (3.4)$$

Finally, the overall turbulence intensity is given by

$$TI = \frac{U_{\text{RMS}}}{\bar{U}} \quad (3.5)$$

The overall turbulence intensity would be particularly useful to compare different operating conditions, of which there is no data for this case. Nonetheless, the purpose here is to establish the grounds from an infodynamic approach one should apply in other cases. Fig. 3.12 depicts the mapping of the overall turbulence intensity where it is possible to identify the likely location of the small vortex upstream of the stagnation point, as argued in Silva et al. (2017), and a second peak at what could be the central region of the ground vortex, on average, with a low-velocity.

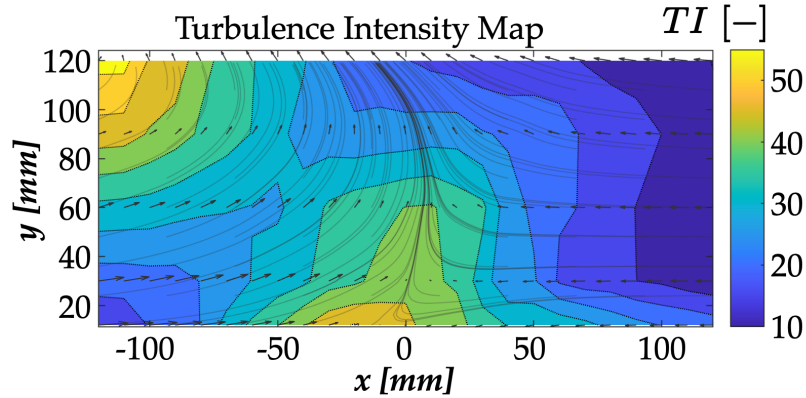


Figure 3.12: Obtained results regarding the global turbulence intensity and the corresponding calculated streamlines.

For the corresponding overall *turbulence intensity infotropy*, considering the relevance of both velocity components, if the information part depended on the distribution of $U_i = \sqrt{u_i^2 + v_i^2}$, the map would be similar to the TI map. Instead, one decided to contextualize the *mutual informature*, defining the *overall turbulence intensity relative infotropy* as

$$H_e^{TI} = TI \cdot \left(\frac{mH_{I,e}(u, v)}{2H_{max,e}} \right) \quad (3.6)$$

considering that the *maximum informature* of u and v is equal. Fig. 3.13 highlights the region of a higher overall degree of transformation above the stagnation point,

3. Infodynamic Analysis of Turbulence in Ground Vortex

suggesting the location of highly coherent structures that depend on a strong correlation between u and v .

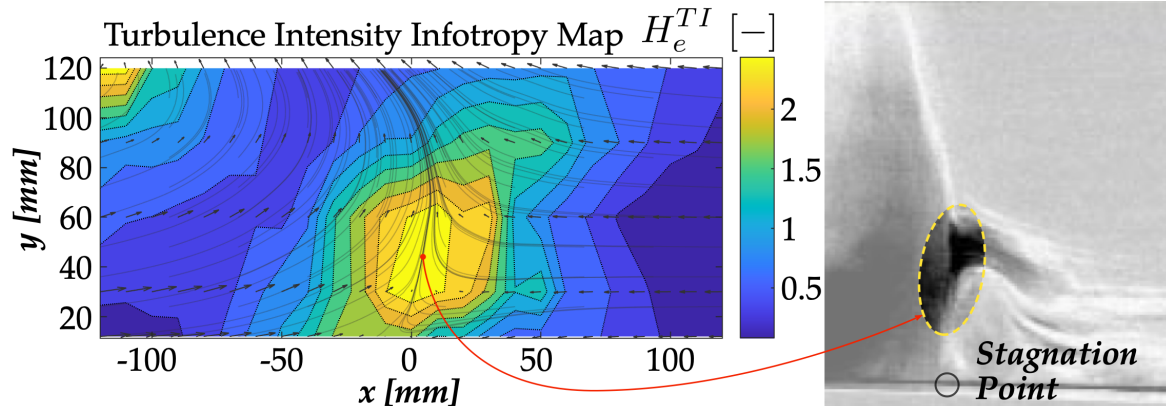


Figure 3.13: Obtained results regarding the overall turbulence intensity infotropy and the corresponding calculated streamlines.

On the right side is the identification of the structure present in the visualizations, linked with the main region of growth, development, and detachment of a secondary vortex formed on the wall. This result also emphasizes that an infodynamic analysis of turbulent flows is not an alternative to more conventional analysis, for example, based on the turbulence intensity, but shows an additional perspective, where the explorations made in this dissertation are only the first step.

A final comment regards the practical significance of the infodynamic analysis compared to a conventional statistical analysis or those based on the conservation of mass, momentum, and energy. The essential element in infodynamics is information. Furthermore, similarly to a thermocouple that measures temperature through the Seebeck effect, an *infosensor* measures *informature* through the relative frequencies obtained statistically. It is important to note that there is no competition between all the statistical analyses done so far of turbulent flows and the infodynamic analysis. Also, infodynamics includes information as a fourth element besides mass, momentum, and energy used to describe and understand turbulent flows. However, while some analyses map the structures based on estimations of Reynolds stresses, vorticity, or energy spectra, infodynamics identifies structures from the stochasticity inside the raw data treated statistically to obtain relative frequencies. In a sense, there is still some creative phase space in how one expresses the relative frequencies of turbulent flow characteristics. For example, a binarization of the velocity signal with the value of 1 for $d\phi/dt > 0$ and 0 for $d\phi/dt \leq 0$ would produce a different message retrieved for a turbulent flow. The ongoing work on defining messages and corresponding relative frequencies for further infodynamic analysis holds great promise for the future.

4. Conclusions and Future Work

The nature of a turbulence flow is its indeterminacy. While typical analysis of turbulence include the conservation of mass, momentum, and energy, this dissertation explores a fourth less known perspective: information. In information theory, the amount of information of a non-deterministic system is the average degree of surprisal measured through the relative frequencies of all possible values for a certain characteristic of this system. Given the stochastic nature of turbulence, the objective of this dissertation is to apply an infodynamic analysis to study the informational content of physical phenomena in turbulent flows. In this sense, one uses the studied case of a vertical/short take-off and landing aircraft, where the collision between a wall jet and a boundary layer results in an upwards-curved flow to investigate its informational content. This turbulent flow was associated with losses by instabilities originating from three main structures: a ground vortex, a small vortex, and a secondary vortex.

After clarifying the principles from information theory adapted to a novel practical engineering-orientated lexicon, the infodynamic analysis evaluates whether or not information offers a fresh perspective in the analysis of the pre-explained physical phenomena. The introduced terms like *informature*, which quantifies the amount of information in a physical system with a non-deterministic nature, as well as *infotropy* which contextualised informature, and *infosensor*, an instrument or measurement technique able to capture enough information to measure informature through statistical analysis principles, where all used to innovatively measure the transformations within the flow field under analysis.

The infodynamic analysis revealed behaviours of turbulent structures that a classical time-integrated statistical analysis, using mean values and mean velocity fluctuations, is unable to capture. The *informature* maps not only reveal the position of high variability related to the epicenter of the ground vortex, but also the area affected by the rupture of the increasing vorticity resulting from the growth and development of a small vortex into a secondary one, followed by its detachment and convection by the main ground vortex. Additionally, the *mutual informature* map shows that the vertical and horizontal components of velocity are related, highlighting the importance of their simultaneous measurement in the study of this type of turbulent flows. It is also observed that when *infotropy* is contextualized by turbulence intensity, the existence of the secondary vortex is confirmed in a region of high degree of transformation above the stagnation point. In this way, the limitations of turbulence intensity by the intensifying the effect of low mean velocities are overcome. These results suggest the *turbulence intensity relative infotropy* as a better or complementary metric to turbulence intensity.

Overall, this study demonstrates the effectiveness of the novel information theory lexicon applied to engineering physical systems. By providing new and significant insights into the investigated flowfield, this approach offers a transformative perspective

for understanding complex engineering processes that encompass both deterministic and non-deterministic elements. Therefore, its broader application in future studies is recommended. To further our understanding of turbulence and the behaviours of this new information theory lexicon, which is still in its early stages of development, an experimental setup is already being designed. This experimental setup will analyze the stochastic nature of turbulence in a two-phase flow (ultrasonic spray plume) by processing the informational content of the flow before and after different object shapes.

Bibliography

- Abbaszadeh, M., Huang, Y., Thomas, P. J., Wen, M., Ji, F., and Guo, W. (2021). Kolmogorov turbulence and information dissipation in molecular communication. *IEEE Transactions on Molecular, Biological and Multi-Scale Communications*, 7(4):262–270.
- Barata, J., Ribeiro, S., Santos, P., Silva, A., and Silvestre, M. (2008). Experimental study of instabilities and secondary effects of a ground vortex flow. In *46th AIAA Aerospace Sciences Meeting and Exhibit*, page 343.
- Ben-Naim, A. (2017). *Information theory: part I: an introduction to the fundamental concepts*, volume 1. World Scientific.
- Bendat, J. S. and Piersol, A. G. (1966). *Measurement and analysis of random data*. Wiley.
- Cerbus, R. T. (2014). *Information perspective on turbulence*. PhD thesis, University of Pittsburgh.
- Denbigh, K. (1981). How subjective is entropy? *Chemistry in Britain*, 17:168.
- Granero-Belinchón, C., Roux, S. G., and Garnier, N. B. (2018). Kullback-leibler divergence measure of intermittency: Application to turbulence. *Physical Review E*, 97(1):013107.
- Leonenko, N., Pronzato, L., and Savani, V. (2008). A class of Rényi information estimators for multidimensional densities. *The Annals of Statistics*, 36(5):2153 – 2182.
- Lozano-Durán, A. and Arranz, G. (2022). Information-theoretic formulation of dynamical systems: causality, modeling, and control. *Physical Review Research*, 4(2):023195.
- Lumley, J. and Yaglom, A. (2001). A century of turbulence. *Flow, Turbulence and Combustion*, 66:241–286.
- Mehta, R. D. and Bradshaw, P. (1979). Design rules for small low speed wind tunnels. *The Aeronautical Journal*, 83(827):443–453.
- Panão, M. O. (2024). Infodynamic measurement science. *Measurement Science and Technology*. (Under Preparation).
- Panão, M. R., Ferrão, I., and Moita, A. S. (2024). Is biofuel HVO an alternative in aviation? An Infodynamic Comparative Analysis. In *21st International Symposium on the Application of Laser and Imaging Techniques to Fluid Mechanics*, page 25pp., Lisbon, Portugal.

- Passaggia, P.-Y., Mazellier, N., and Kourta, A. (2021). Aerodynamic drag modification induced by free-stream turbulence effects on a simplified road vehicle. *Physics of Fluids*, 33(10).
- Shannon, C. E. (1948). A mathematical theory of communication. *The Bell System Technical Journal*, 27(3):379–423.
- Silva, A. R., Panão, M. R., and Barata, J. M. (2017). On the use of finite mixtures to improve the physical interpretation of a ground vortex flow. *Experimental Thermal and Fluid Science*, 85:344–353.
- Stone, J. V. (2015). *Information theory: a tutorial introduction*. Sebtel Press.
- Tribus, M. and McIrvine, E. C. (1971). Energy and information. *Scientific American*, 225(3):179–190.
- Tseng, L.-C., Huang, R. F., and Chen, C.-C. (2010). Significance of face velocity fluctuation in relation to laboratory fume hood performance. *Industrial health*, 48(1):43–51.
- Yap, T., Abdullah, M., Husain, Z., Ripin, Z. M., and Ahmad, R. (2001). The effect of turbulence intensity on the aerodynamic performance of airfoils. In *4th International Conference on Mechanical Engineering*, pages 31–36.

A. Laser Doppler Velocimetry System Details

All details can be found in Barata et al. (2008). The wind tunnel facility was designed in accordance with the recommendations outlined in Mehta and Bradshaw (1979) for open circuit wind tunnels, with a specific focus on the boundary layer aspect of the flow. Fig. 3.1 illustrates the main elements of the ground vortex flow. A fan of 15 kW nominal power drives a maximum flow of 3000 m³/h through the boundary layer and the wall jet tunnels with exit sections of 300 × 400 mm and 15 × 400 mm, respectively.

A Laser Doppler Velocimetry (LDV) non-intrusive technique characterized the velocity distribution. The LDV system is a DANTEC Flow Lite dual-beam, backscatter laser anemometer, sensible to the flow direction provided by light-frequency shifting from acoustic-optic modulation - the Dantec Flowlite 2D. This device comprises a 10 mW He-Ne and a 25 mW diode-pumped frequency-doubled Nd:YAG lasers, with a $f_s = 40$ MHz frequency shifting induced by Bragg cell in one of the two laser beams to distinguish the velocity direction in the Doppler signal emitted by the light scattering from the seeding particles. The transmission and backward-scattered light collection is made with a focal lens of 400 mm. A half-angle between the beams was set to 2.8° and the calculated dimensions of the axis of the measuring ellipsoid volume at the e^{-2} intensity locations are $135 \times 6.54 \times 6.53 \mu\text{m}$ and $112 \times 5.46 \times 5.45 \mu\text{m}$, for the He-Ne and Diode lasers, respectively. The principal characteristics of the LDV are summarized in Table A.1.

Table A.1: Principal characteristics of the Laser-Doppler Velocimeter

Laser	He-Ne	Diode Laser
Wavelength, λ [nm]	633	532
Focal length of focusing lens, f [mm]	400	400
Beam diameter at e^{-2} intensity, [mm]	1.35	1.35
Beam spacing, s [mm]	38.87	39.13
Calculated half-angle of beam intersection, θ	2.78°	2.8°
Fringe spacing, δ_f [μm]	6.53	5.45
Velocimeter transfer constant, K [MHz/(ms ⁻¹)]	0.153	0.183

The horizontal, U , and vertical, V , mean and turbulent velocities together with the shear stress, $\overline{u'v'}$ were determined by a two-velocity channel Dantec BSA F60 processor. To visualize the flow and perform the LDV measurements, glycerin particles of 0.1 to 5 μm produced with medical atomizers operating at 1.5 bar were used to seed the flow. The transmitting and collecting optics are mounted on a three-dimensional transverse unit, positioning the control volume within ± 0.1 mm.



Figure A.1: Photograph of the experimental rig by Barata et al. (2008).